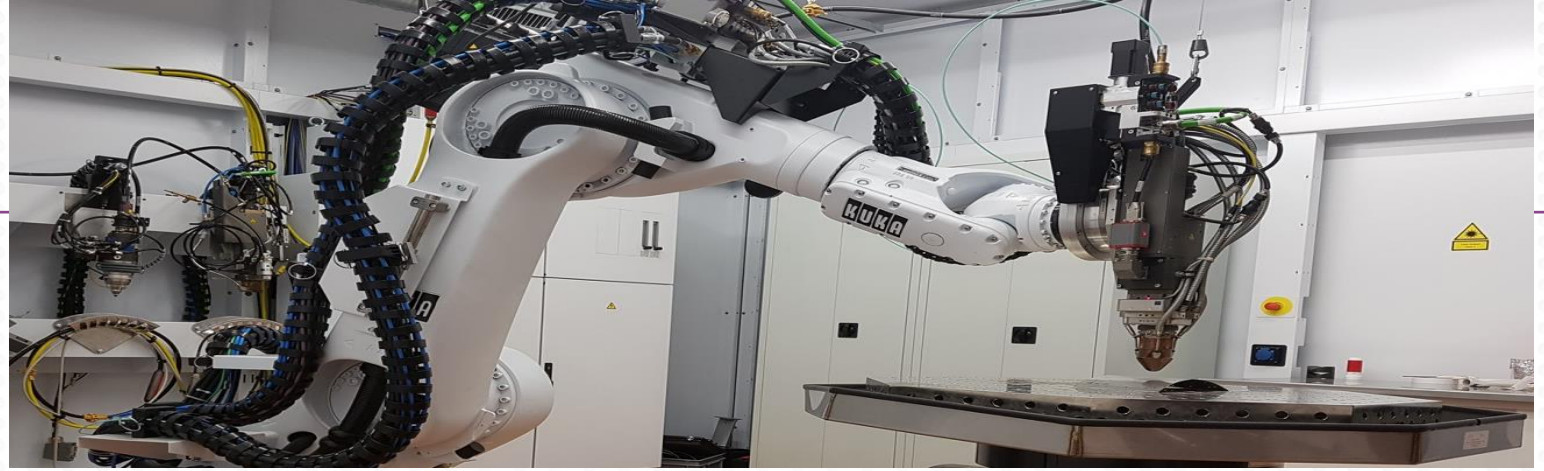

Direct (laser) energy deposition: experimental results vs modellization

Ion N. Mihailescu[1,*], Muhammad Arif Mahmood[2], Asif Ur Rehman[3], Cristian N. Mihailescu[1], Mihai Oane[1], Carmen Ristoscu[1], Sinziana Andreea Anghel[1,4], Andrei C. Popescu[1], Diana Chioibasu[1]

1. *National Institute for Laser, Plasma and Radiation Physics (INFLPR), Magurele-Ilfov, 077125, Romania*
2. *Intelligent Systems Center, Missouri University of Science and Technology, Rolla, MO, 65409, USA*
3. *CY Advanced Studies, CY Cergy Paris Université, Paris, 95000, France*
4. *Faculty of Physics, University of Bucharest, Magurele-Ilfov, 077125, Romania*

Email: ion.mihailescu@inflpr.ro

Motivation

- **ADDITIVE MANUFACTURING (AM)** - *the process of joining materials to make objects from 3D model data, usually layer upon layer*
- **AM** - official industry standard term (ASTM F2792) for all applications of the technology
- **AM** applications are limitless in order to meet diverse needs: visualization tool in design, means to fabricate highly customized products for professionals and everyday consume, industrial tooling to produce small lots of production parts, one day … production of human organs
- AM carried out under laser irradiation = **Laser Additive Manufacturing (LAM)**

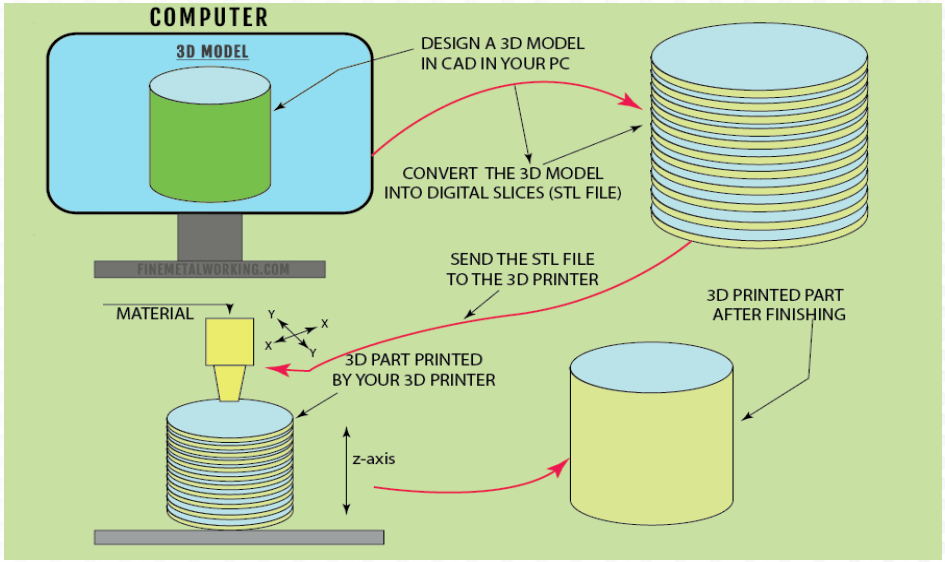

Additive manufacturing process schematic [Ref. Fine metal working]

Classification of LAM Processes

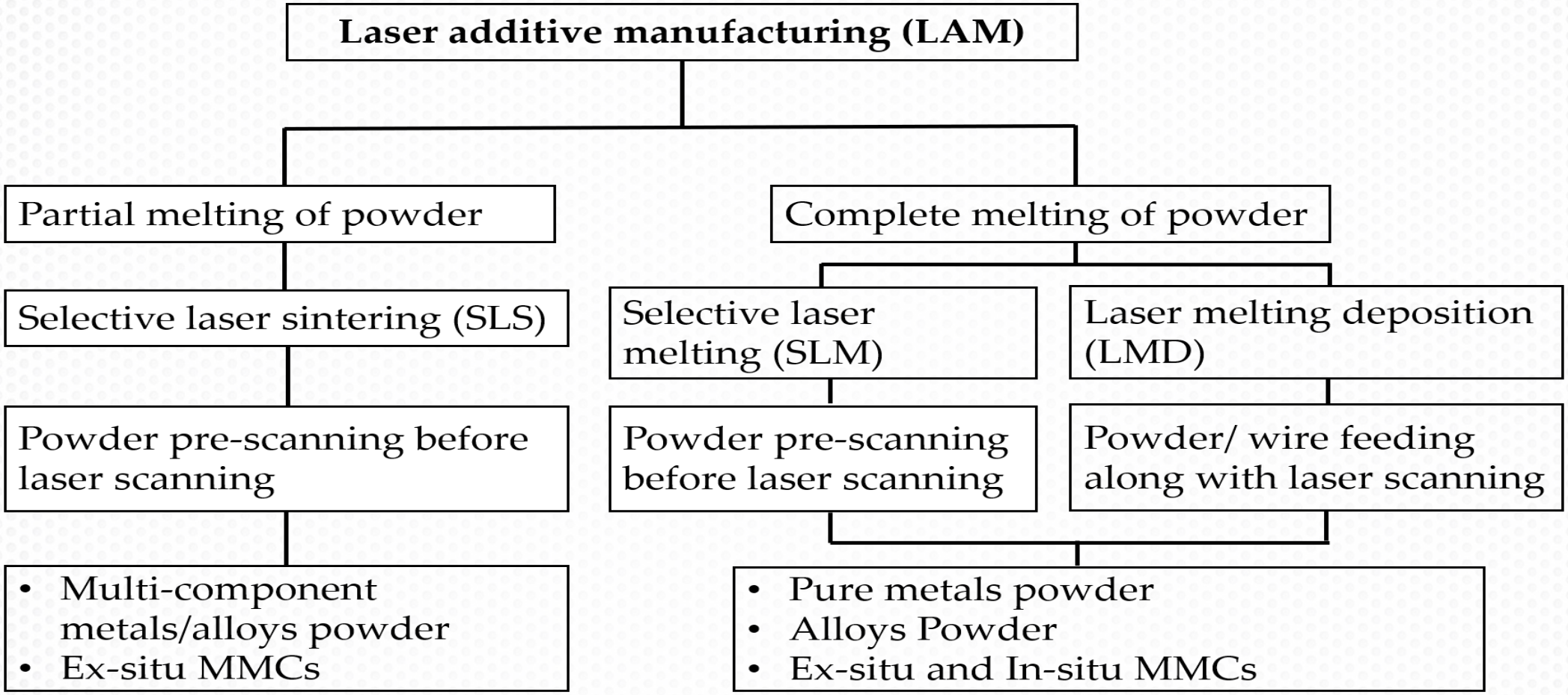

∴ MMC = Metal Matrix Composites

Working Principle of Laser Melting Deposition (LMD)

- **LMD** - economically viable and innovative approach to repair or manufacture fully functional, geometrically complex, and dense parts
- **LMD** - strong candidate for aerospace, automobile, industrial, and biomedical applications

- The simultaneous addition of powder consumes a fraction of the laser beam, while another portion is absorbed by the substrate to generate a melt pool
- The rest of the laser energy is reflected by the substrate
- The powder debits are feed directly into the melt pool, resulting in the clad formation

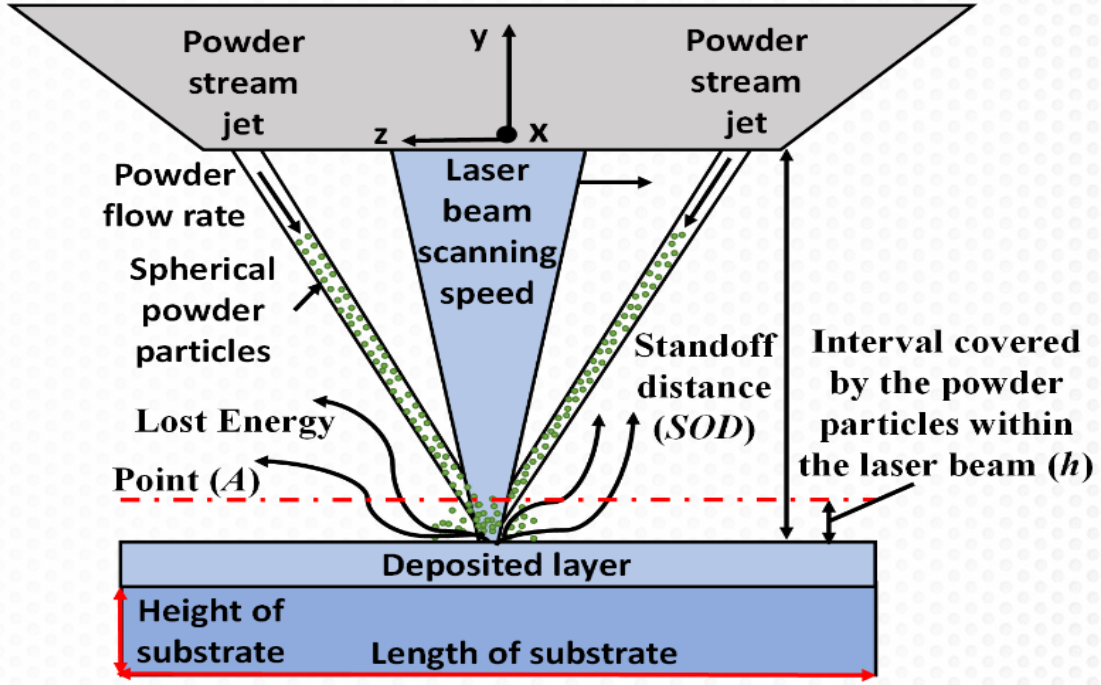

Scheme of the laser beam interaction with a stream of powder particles and substrate

Process parameters for LMD

Operating parameters can be classified into two major categories:

- Controllable parameters (directly from machine)
- Un-controllable parameters (based on controllable parameters)

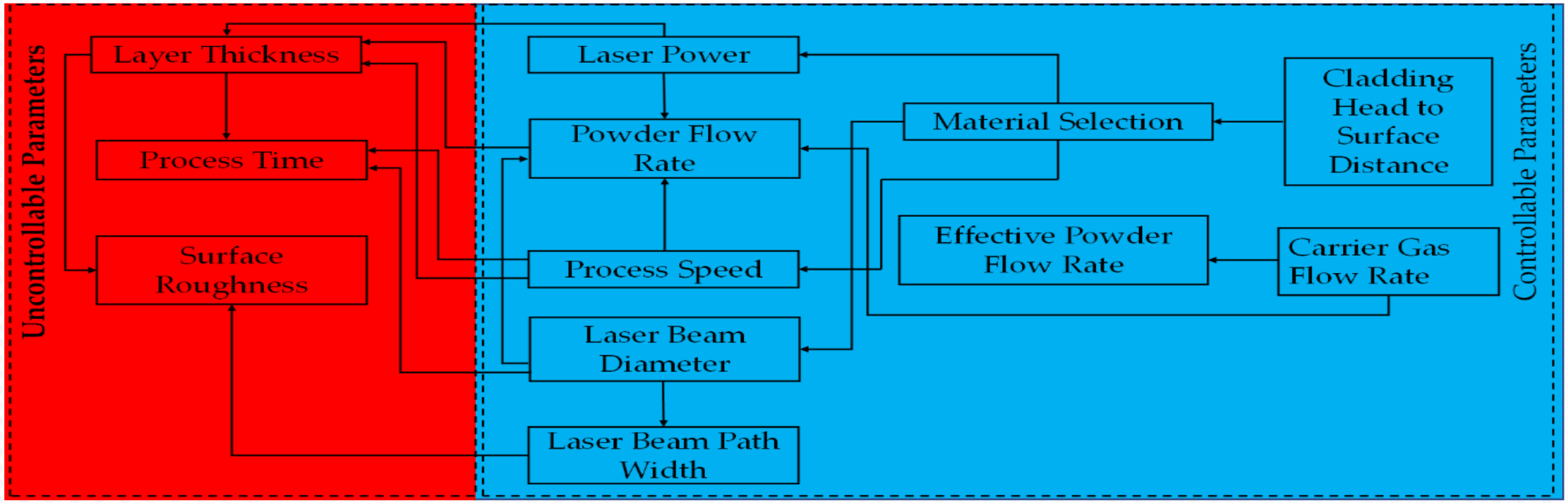

Types of nozzles in LMD equipment

- With a three-/four-jet nozzle, a substantial part of the powder particles that hit the melt pool surface is rebounded
- With a co-axial nozzle, almost all particles are caught in the melt pool
- This is due to the different particle velocities achieved with the two different nozzles

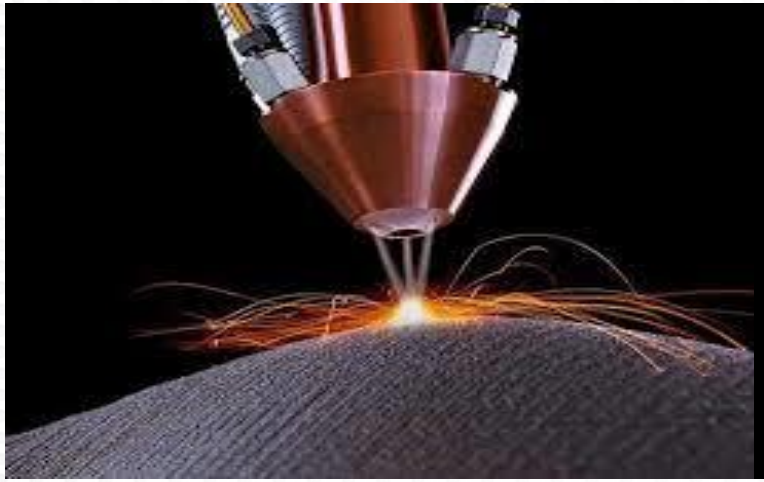

Three-jet powder nozzle

Source: Trumpf Kuka, Kr30HA, Germany

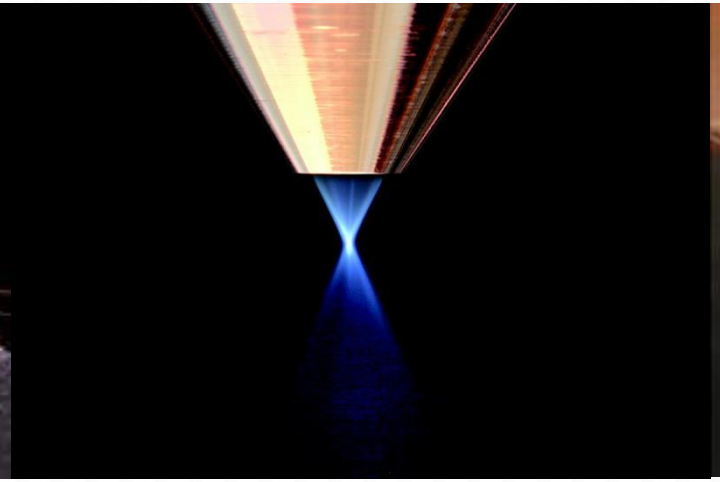

Co-axial powder nozzle

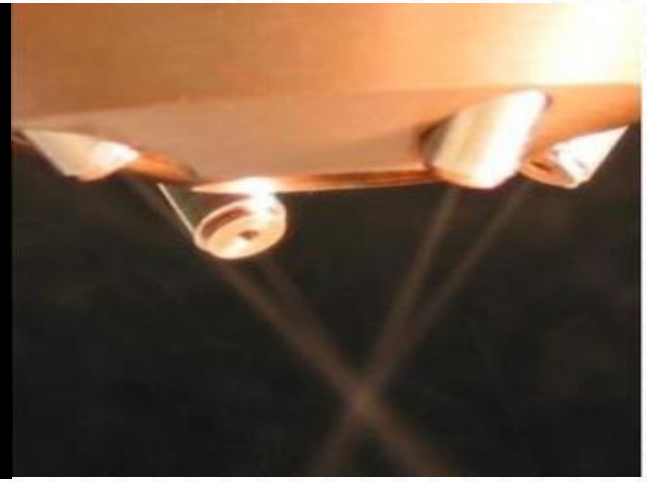

Four-jet powder nozzle

Source: Fraunhofer Institute for Laser Technology ILT, Germany

LMD: Advantages vs. Disadvantages

Advantages:

- Repairing (cladding) and 3D printing of simple and complex parts
- Fabrication of highly dense and near-net shaped parts
- Lower porosity
- Heat affected zone smaller than in SLM and SLS: material strength not affected
- Part distortion inferior to other LAM techniques

Disadvantages:

- Resolution and wall-thickness cannot be controlled
- Mechanical properties anisotropy due to steep thermal gradients
- Properties hard to predict due to large number of process parameters
- Thermal history depends on process parameters
- Intricate process parameters' effects on microstructure with strong dependence on material feed-stock

Why modelling is necessary for LMD processing?

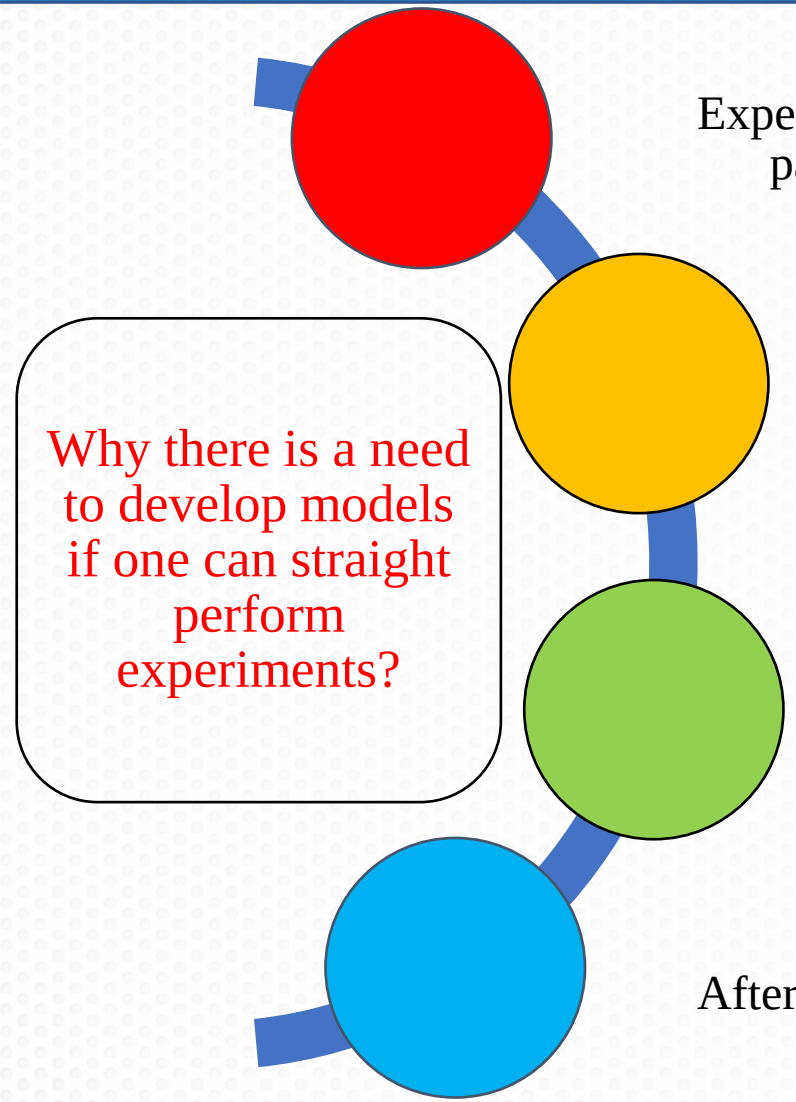

Why there is a need to develop models if one can straight perform experiments?

Experimentation involves a variety of operating parameters which are difficult to control

Modelling helps to understand the one-to-one relation between input and output parameters

Modelling is an inexpensive approach in comparison to experimentation

After modelling, estimation can be done quickly and cost-effectively

Clad Geometry and Residual Stress Distribution

Mathematical models:

- The 1st deposited layer parameters were calculated based on actual operating conditions
- Ahatch spacing was used to assess re-melting depth and other key dimensions for *n* printed layers
- This solution was further used as an input to evaluate the residual stresses inside substrate and deposited layers

Mahmood, M.A., Popescu, A.C., Hapenciuc, C.L. et al. Estimation of clad geometry and corresponding residual stress distribution in laser melting deposition: analytical modeling and experimental correlations. Int J Adv Manuf Technol 111, 77–91 (2020). https://doi.org/10.1007/s00170-020-06047-6

Stress Formation and Accumulation (1)

Thermal gradient mechanism (TGM):

- Produced due to the large temperature variation around the laser spot
- Rapid heating with slow conduction generates a sharp temperature gradient
- Material strength decreases with temperature rise
- Material beneath the heated/deposited layer causes compressive stress-strain

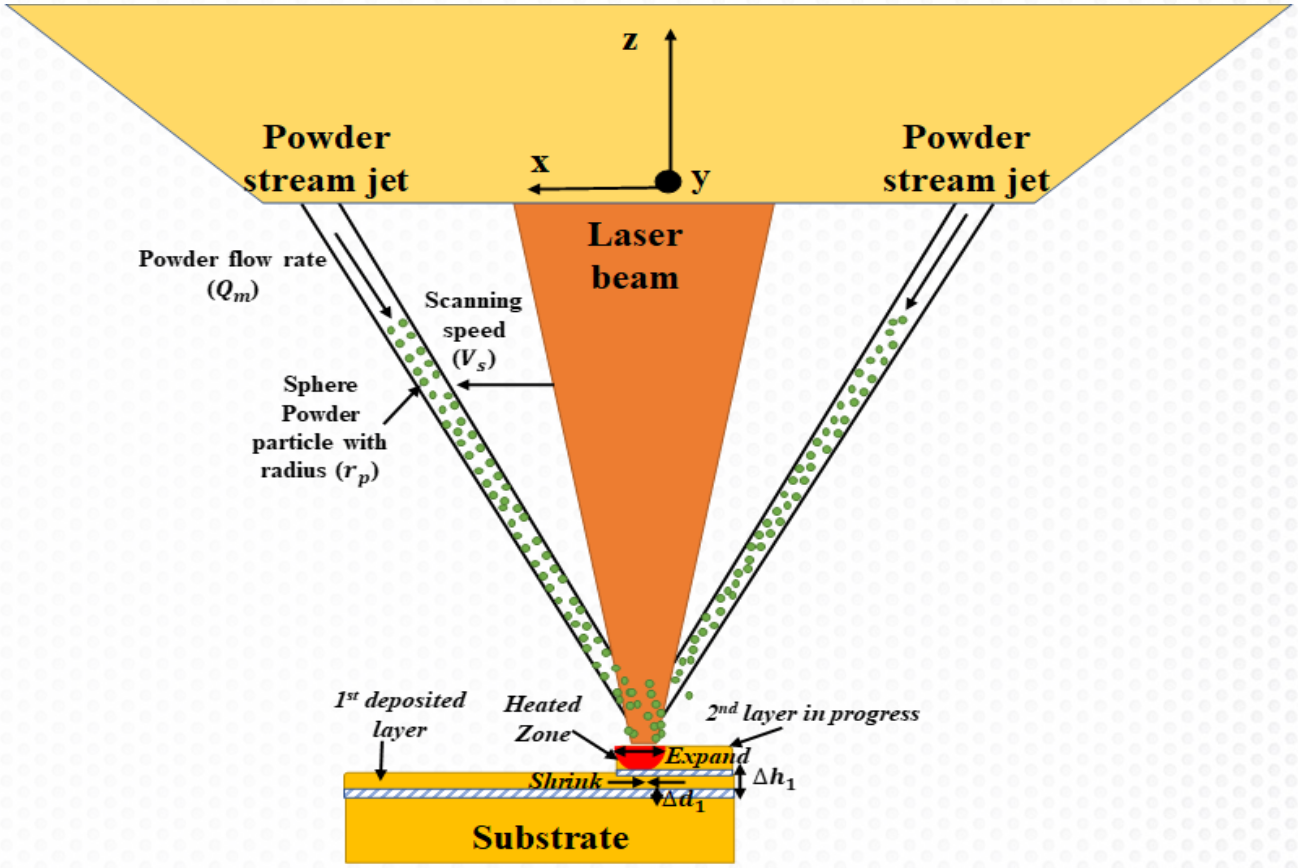

Stress Formation and Accumulation (2)

Cool-down mechanism (CDM)

- The laser beam moves away from the irradiated region, which starts to cool down, causing shrinkage
- The underlying material counteracts and induce tensile stress distribution in the newly added deposit and compressive stress below the freshly deposited layer

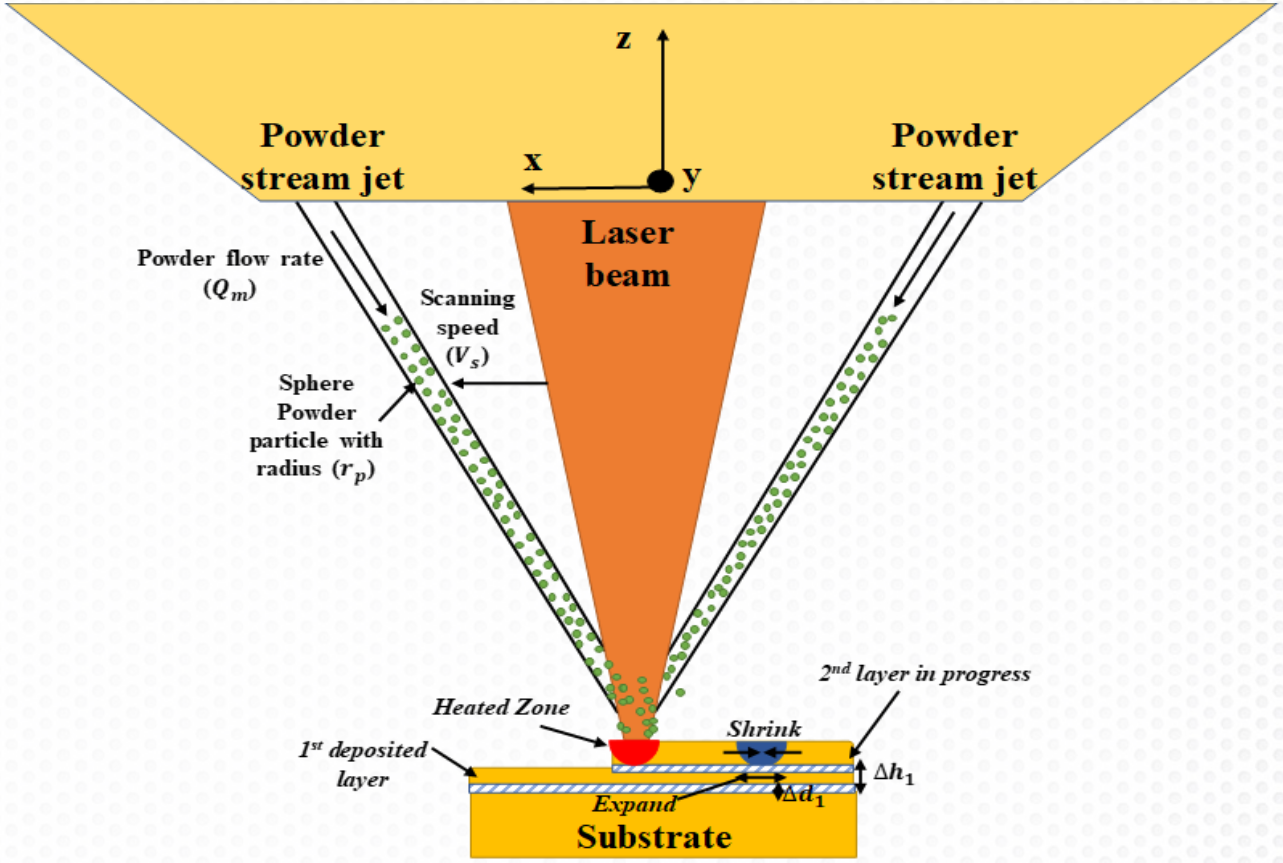

Modelling Strategy

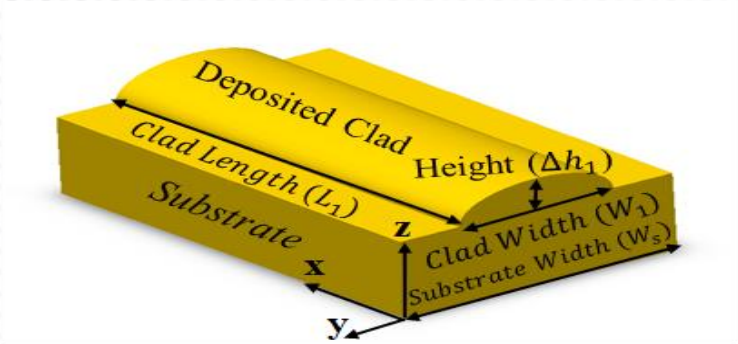

Estimation of clad geometry for single layer

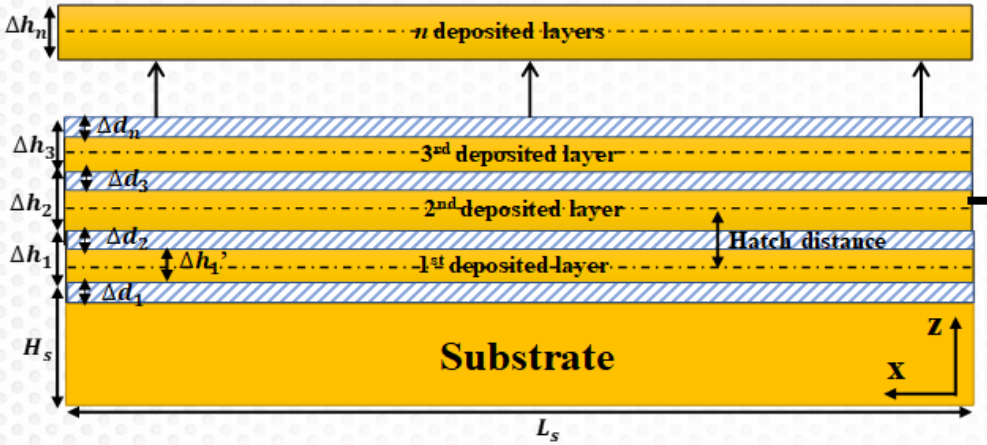

Total clad geometry using hatch distance and re-melting depth

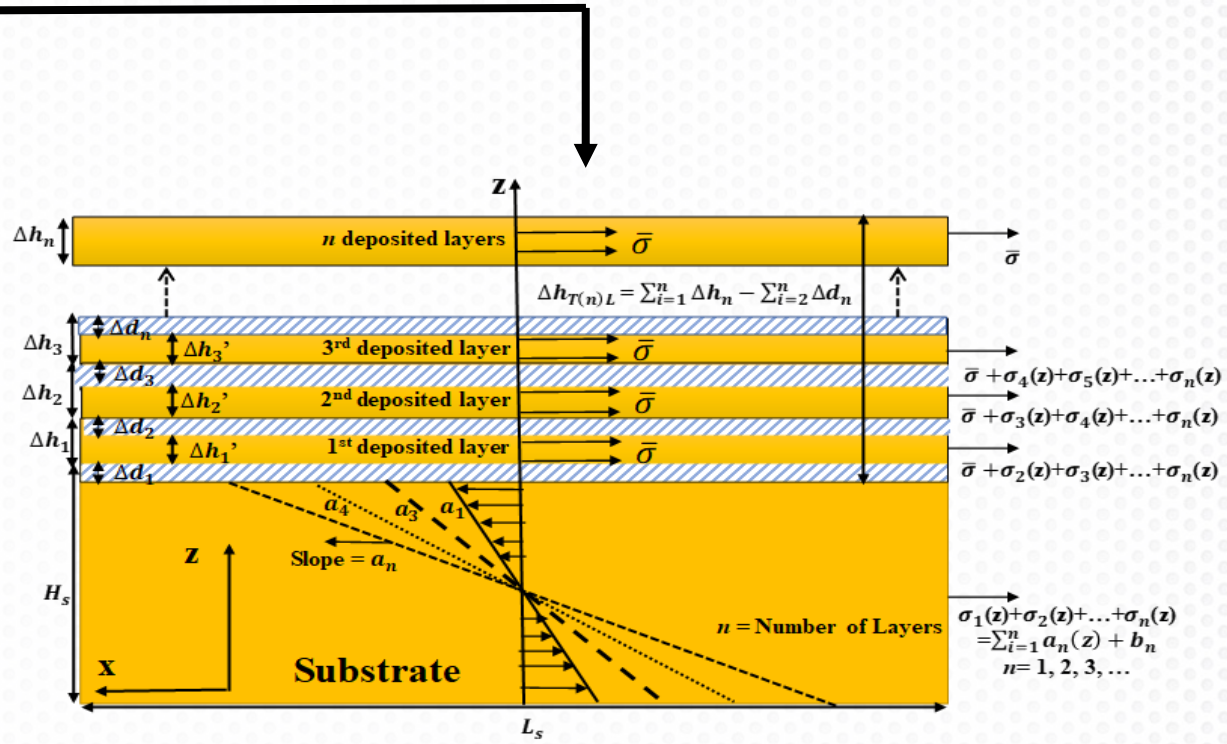

Total stress build-up in LMD

1. Conservation and energy laws
2. Modified value of specific heat and fusion enthalpy

Model validation: 1st clad formation

Experimental data for AISI316L powder on AISI321 bulk substrate from: Rapid Prototyp J 24:270–275 (2016) https://doi.org/10.1108/RPJ-03-2015-0027

Case number	Power (W)	Powder feed rate (g/s)	Laser scanning speed (mm/sec)	N:Parameter	Value
01	624	0.078	2.17	Stand off distance	20 mm
02	1063	0.133	3.69	Material density (substrate/powder)	8027 / 8000 kg/m^3
03	1495	0.187	5.19	Laser spot size	1.5 mm
04	1927	0.241	6.72	Laser absorption (substrate/powder)	0.40 / 0.16
05	2358	0.295	8.19	Specific heat (substrate/powder)	500/500 J/kg.K
06	2790	0.349	9.69	Powder mean radius	60 µm
07	3222	0.403	11.19	Length of Layer	40 mm
08	542	0.078	2.51	Fusion enthalpy (substrate/powder)	285 / 260 kJ/kg
09	952	0.133	4.29	Melting temperature (substrate/powder)	1446 /1400 °C

Model validation

1st deposited layer dimensions

- Model estimates clad **(a) width, (b) height,** and **(c) depth** with a (10 – 15) % mean absolute error
- Deviations between the experimental and simulation results might be due to surface tension which was assumed negligible
- Powder efficiency equivalent to 40 % was taken into account, which influences the accuracy of the model `

Width

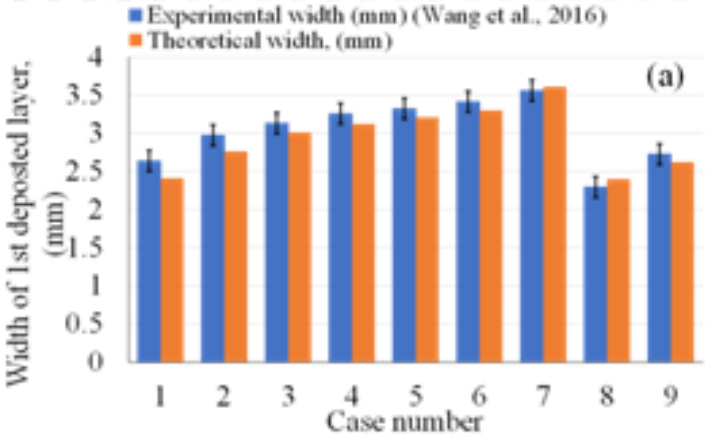

Height

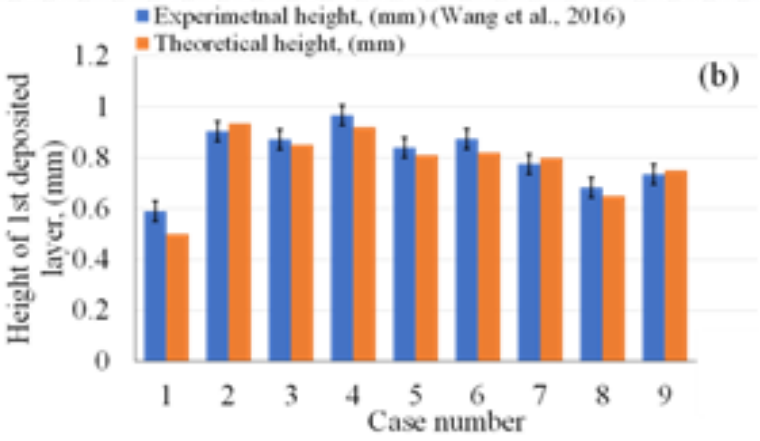

Depth

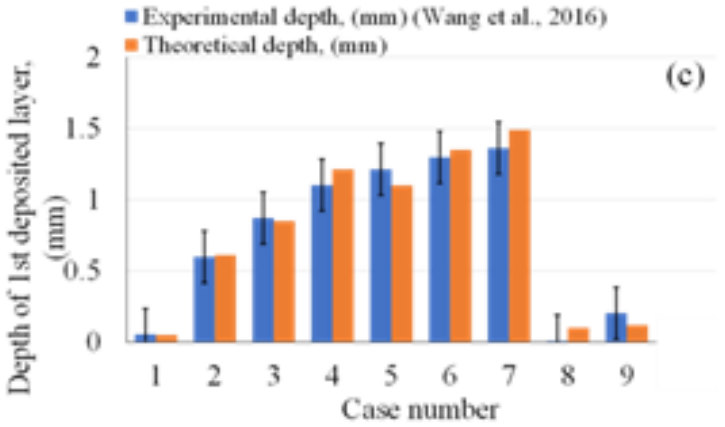

Residual stress

- - model predictions compared with stress measurements by XRD and simulated by Finite Element method (see Note)
- - close correlation between the experimental and analytical modelling results, with a (8 – 14) % mean absolute deviation
- - computing time of ~39 s, far less than the Finite Element-based simulations (2 hrs)

LMD deposited layers-substrate system	Residual measurement method	$\bar{\sigma}$ (MPa)	$(H_s - \Delta d_1)$ (mm)	$h_{T(n)L}$ (mm)	n
AISI 4340 steel-ASIS 4140 steel (Sun et al., 2014)	X-ray diffraction	1200	5	5	3
AISI304 stainless steel-AISI304 stainless steel (Liu, 2014)	Finite element modelling	410	3.175	1.500	3

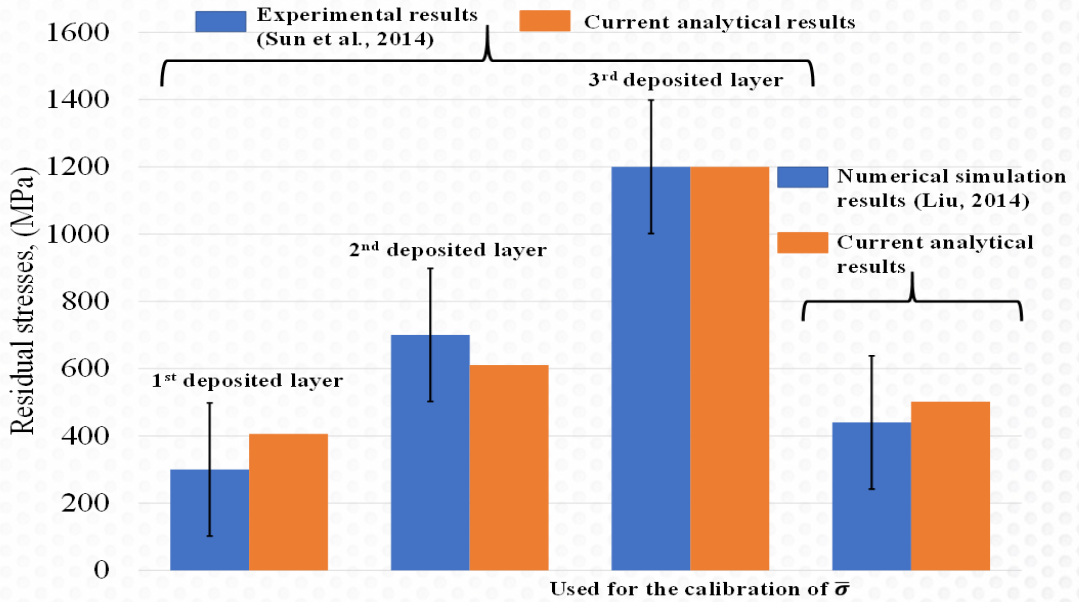

Note:

- ***Sun et al., 2014:*** *Acta Mater 84:172–189. https://doi.org/10.1016/j.actamat.2014.09.028.*
- ***Liu, 2014:*** *Numerical analysis of thermal stress and deformation in multi-layer laser metal deposition process. Masters Theses.*

Three-jet Powder Flow and Effect on Thermal Distribution

Mahmood, M.A.; Popescu, A.C.; Oane, M.; Ristoscu, C.; Chioibasu, D.; Mihai, S.; Mihailescu, I.N. Three-Jet Powder Flow and Laser–Powder Interaction in Laser Melting Deposition: Modelling Versus Experimental Correlations. Metals 2020, 10, 1113. https://doi.org/10.3390/met10091113

Powder flow schematic diagram

- Gravitational effect during powder particle flow is neglected
- Spherical powder particles with normalized size distribution
- Overlapping and collision between powder particles are neglected

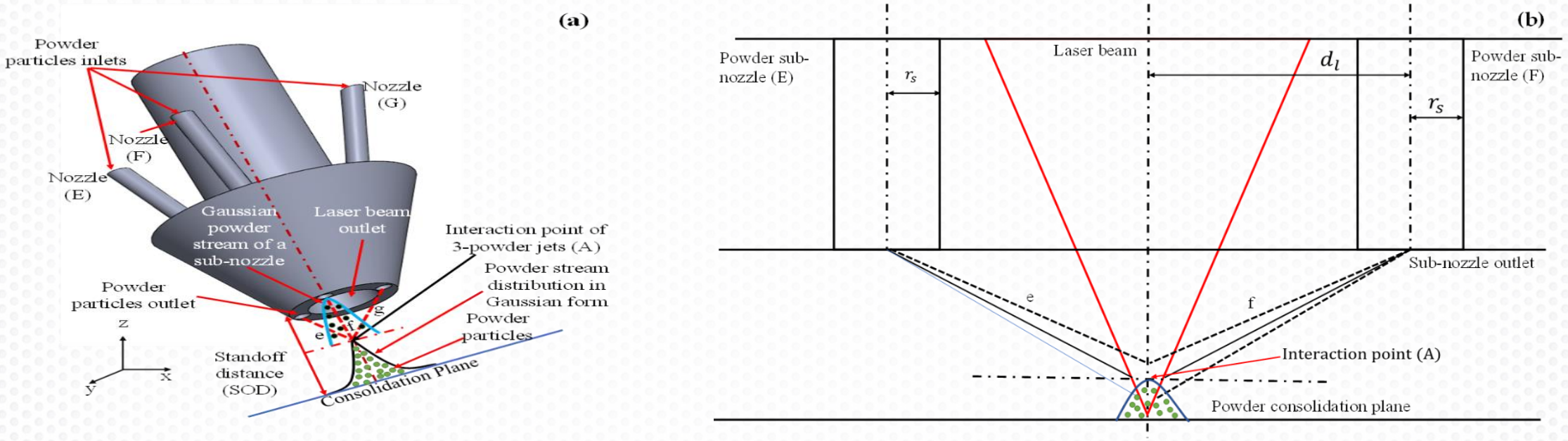

3-jet powder nozzle with a Gaussian powder stream: ***(a)*** *3D and* ***(b)*** *2D representation*

Schematic for Model Development

Three-jet Powder flow

Temperature distribution at the substrate with the addition of powder particles and laser beam attenuation

Phase control of powder particles and substrate with complete melting

Materials and Methods: for comparison with simulation results

Parameter (Units)	Numerical simulations: Fe-TiC on carbon steel substrate	Numerical simulations: 12Cr Ni_2 alloy steel powder on 45 steel substrate	Experiments: Ti6Al4V powder on Ti6Al4V substrate
Laser power (W)	885	1800	400
Scanning speed (mm/s)	2.0	5.0	6.67
Powder feeding rate (g/min)	4.0	11.0	2.5
Powder jet radius (m)	1.30×10^{-3}	1.60×10^{-3}	1.70×10^{-3}
Laser beam radius (m)	1.25×10^{-3}	1.50×10^{-3}	1.05×10^{-3}

Experimental details:

- Nozzle (Trumpf, Ditzingen, Germany) with 3-jet powder stream mounted on a robot (KR30HA, Kuka, Augsburg, Germany) equipped with LMD optics
- High-speed imaging camera (AX100, Photron, Tokyo, Japan)
- 1000 frames per second and shutter speed equal to 1/5000 s to image the powder flow

Experimental and simulation results of three-jet powder flow

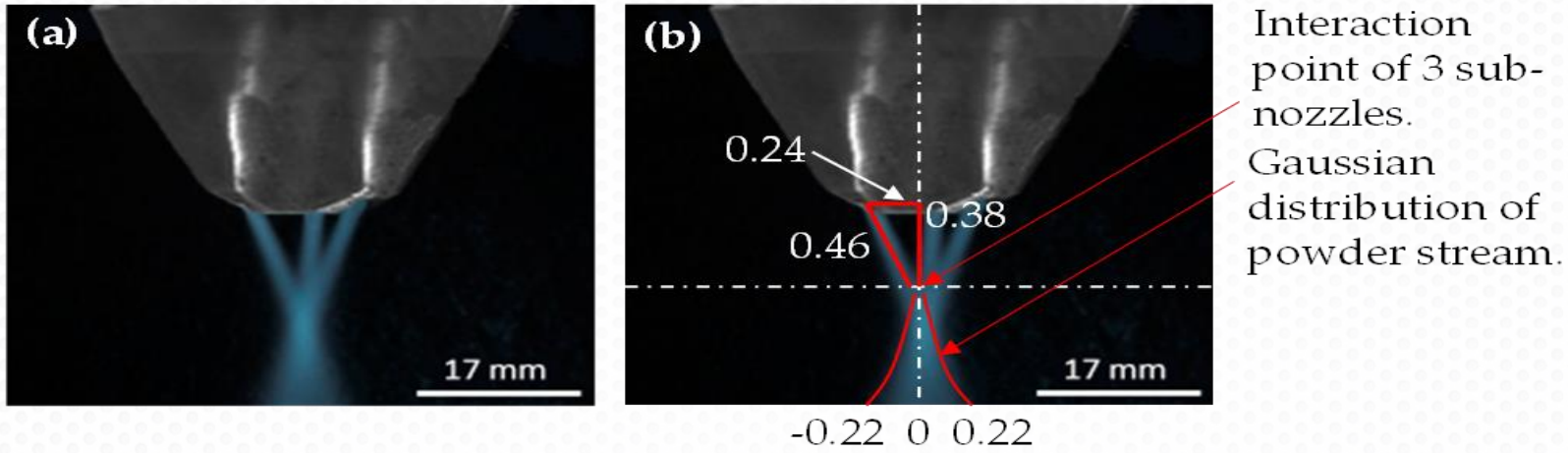

(a) High-speed camera image , (b) image processed with "Image-J" software

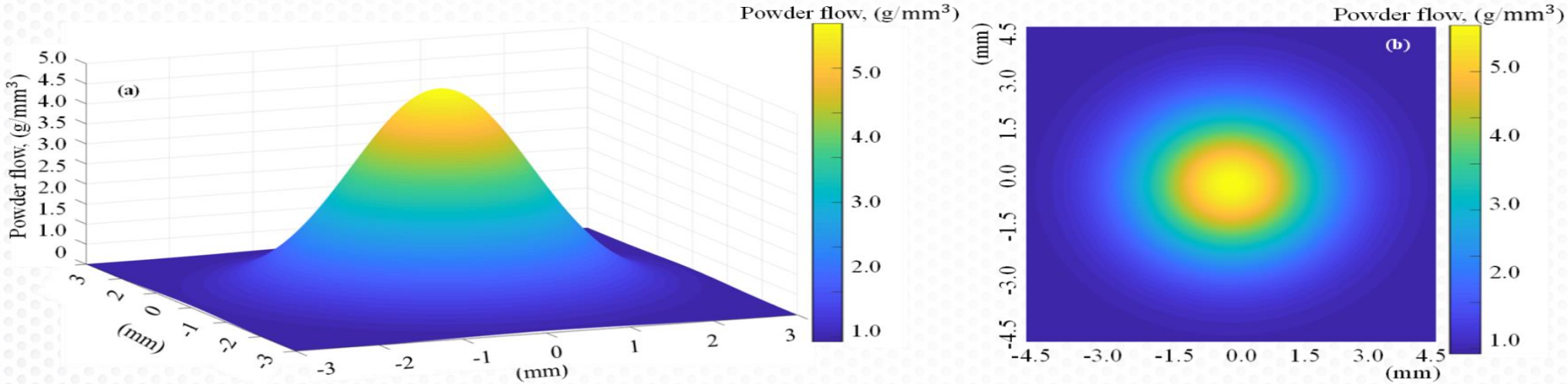

MATLAB plots: (a) 3D, and (b) Contour

Comparison of experimental and simulation powder flows: Effect of focal plane position on powder stream distribution

- Close correlation between experimental and simulation results
- Powder stream follows the Gaussian distribution at the focal plane, (focal plane + 1 mm) distance and (focal plane + 2 mm) distance
- Powder stream shifts from the Gaussian to Transition stream at (focal plane + 2.5 mm)
- Powder flow changes into Annular powder stream at (focus plane + 3 mm)

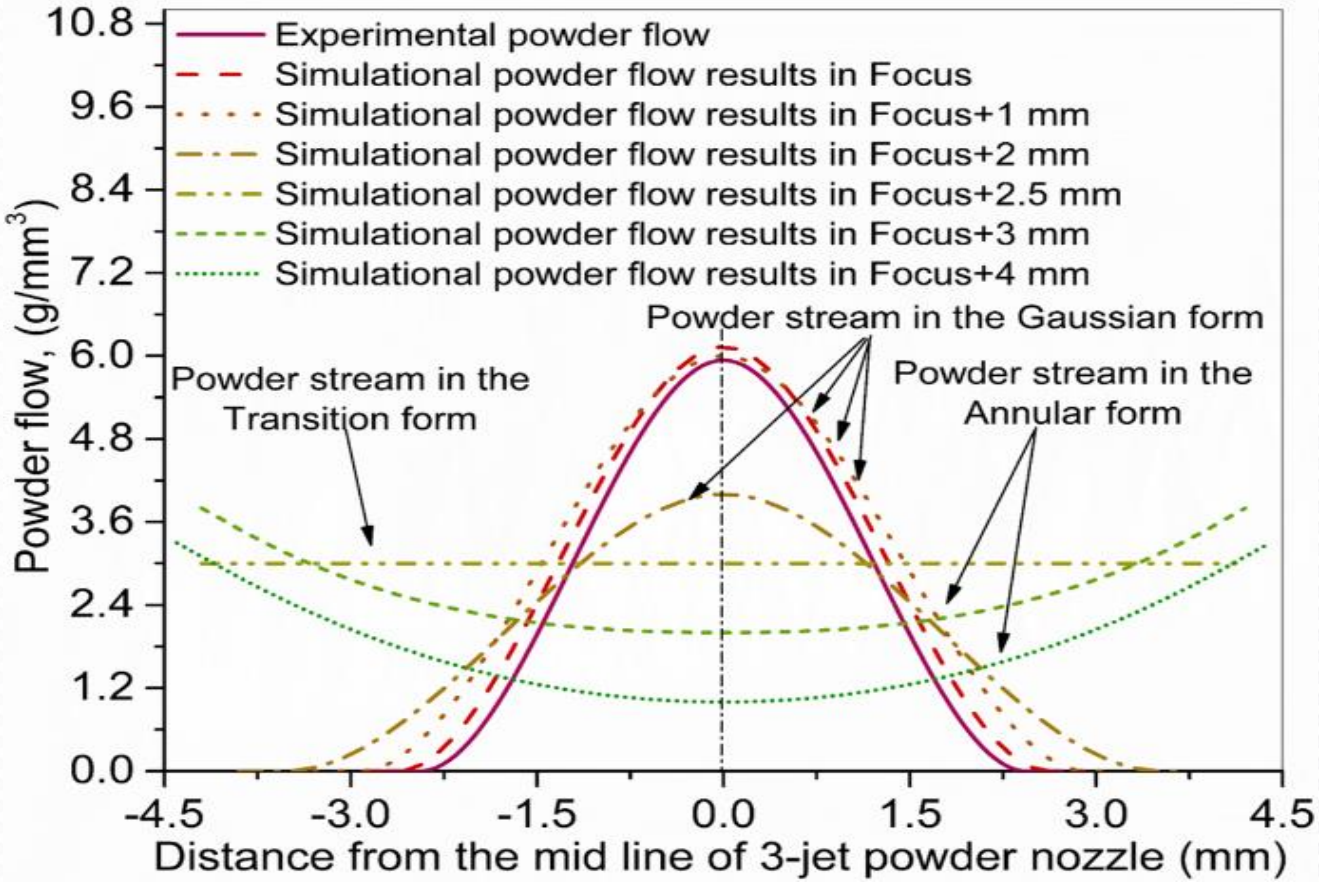

Analytical model comparison with numerical simulation and experimental results

- Close correlation except the absolute mean deviation (≈ 10 %)
- Deviation due to material properties which were considered independent of temperature change, and the usage of a point heat source
- Computing time was approx. 40 s, which is far less than the Finite Element-based simulations (=2.5 hrs).

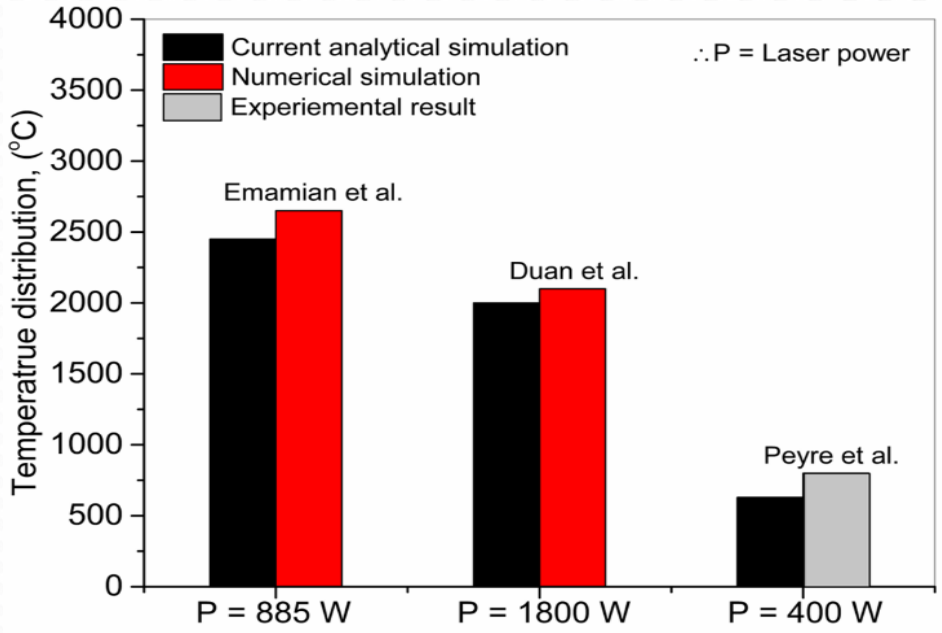

Note:

- ***Emamian et al.:*** *Appl. Surf. Sci.* ***2012****, 258, 9025–9031.*
- ***Duan et al.:*** *Mater. Sci. Eng.* ***2019****, 677 022019*
- ***Peyre et al.:****. J. Laser Appl.* ***2017****, 29, 1–8.*

Effect of laser power, scanning speed and powder addition on temperature distribution

3D Plots

Contour Plots

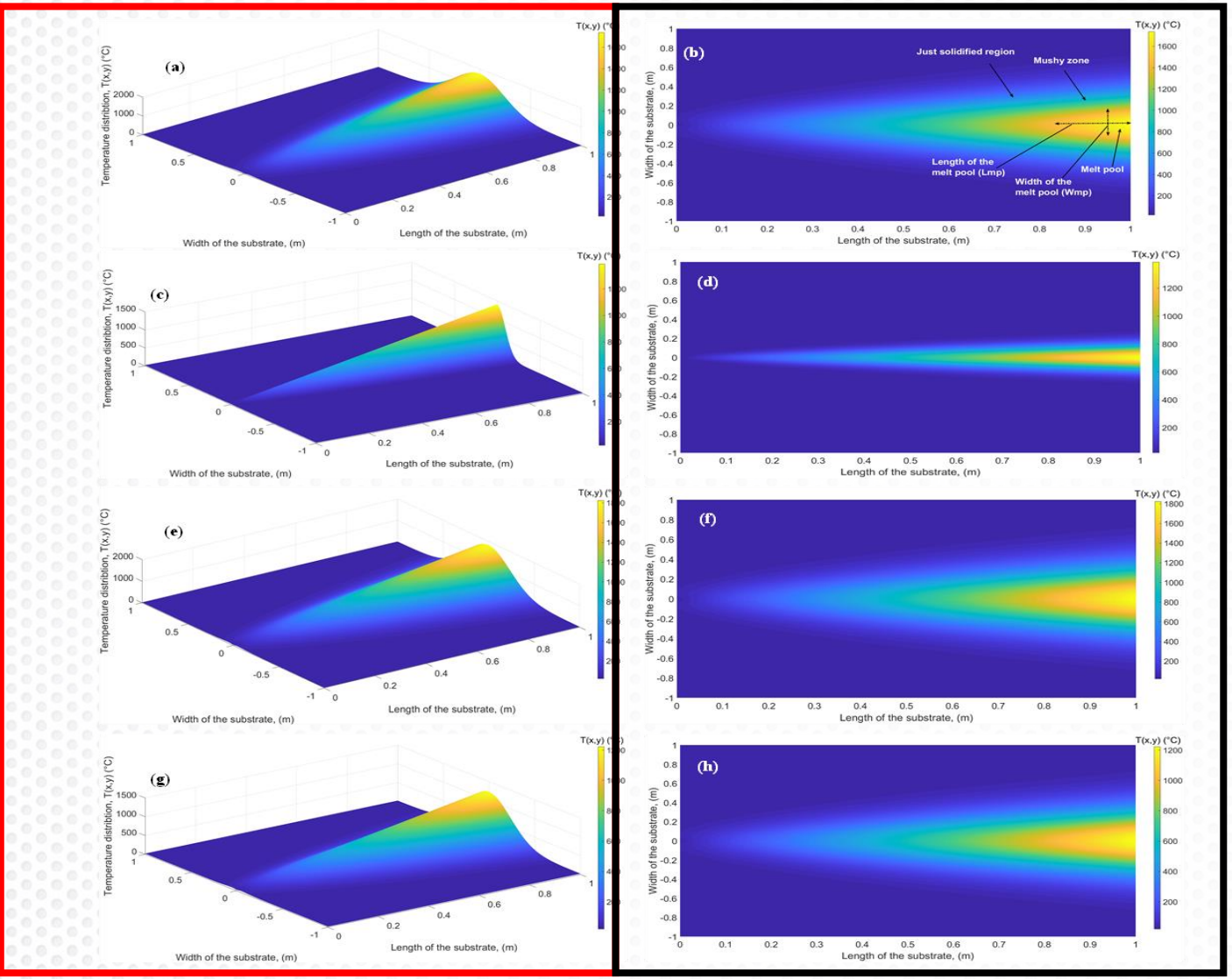

- Three regions can be identified: (1) melt-pool, (2) mushy zone, and (3) just solidified region
- When laser power increases, temperature intensity rises
- When laser scanning speed amplifies, temperature intensity decreases
- When powder feeding rate increases, the temperature intensity at the substrate decreases

Temperature profiles for:

(a) Power (P) = 400 W, scanning speed (v_l)= 0.3 m/min;
(b) 2D plot of (a);
(c) P = 400 W, v_l = 0.35 m/min;
(d) 2D plot of (c);
(e) P = 500 W, v_l = 0.3 m/min;
(f) 2D plot of (e);
(g) P = 400 W, v_l = 0.3 m/min and co-axial powder flow;
(h) 2D plot of (g).

Powder flow and temperature distribution

- A significant amount of powder debits undergoes the laser beam with the increase in powder flow rate
- Energy density used for melting resulting in the temperature drop at the substrate's surface

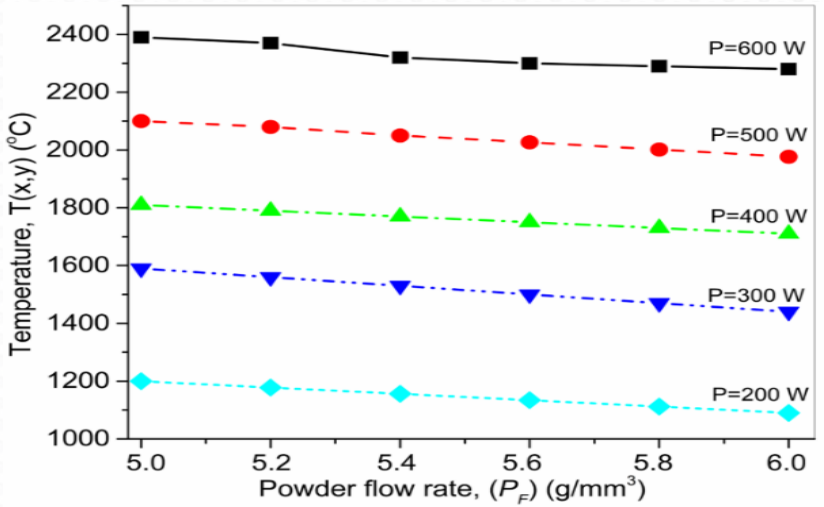

- Gaussian powder stream with maximum average temperature at the substrate
- Powder particles absorb the laser energy during Transition or Annular stream but do not participate in clad formation
- Gaussian powder stream is preferred for optimum LMD

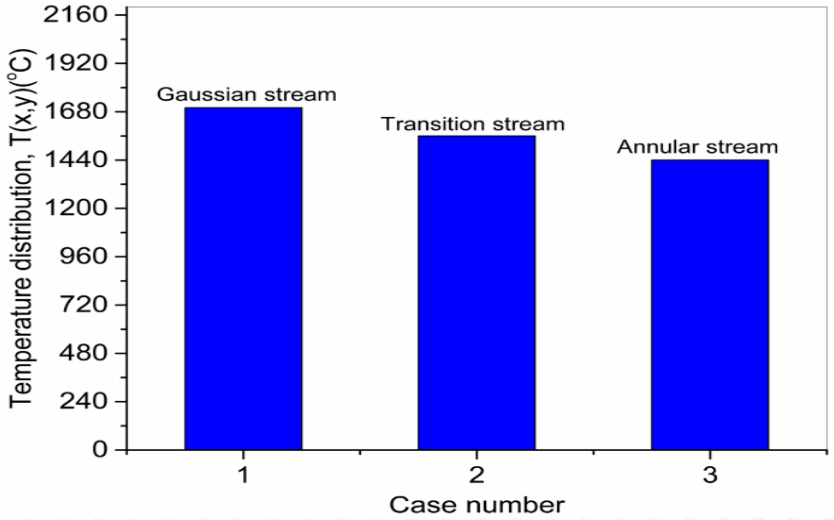

Microstructure Evolution and Corresponding Mechanical Properties

Mahmood, Muhammad Arif & Popescu, Andrei & Oane, Mihai & Diana, Chioibasu & Popescu-Pelin, Gianina & Ristoscu, Carmen & Mihailescu, I.. (2021). Grain Refinement and Mechanical Properties for AISI304 Stainless Steel Single-tracks by Laser Melting Deposition: Mathematical Modelling versus Experimental Results. Results in Physics. 22. 103880. 10.1016/j.rinp.2021.103880.

Laser-melting Deposition Equipment

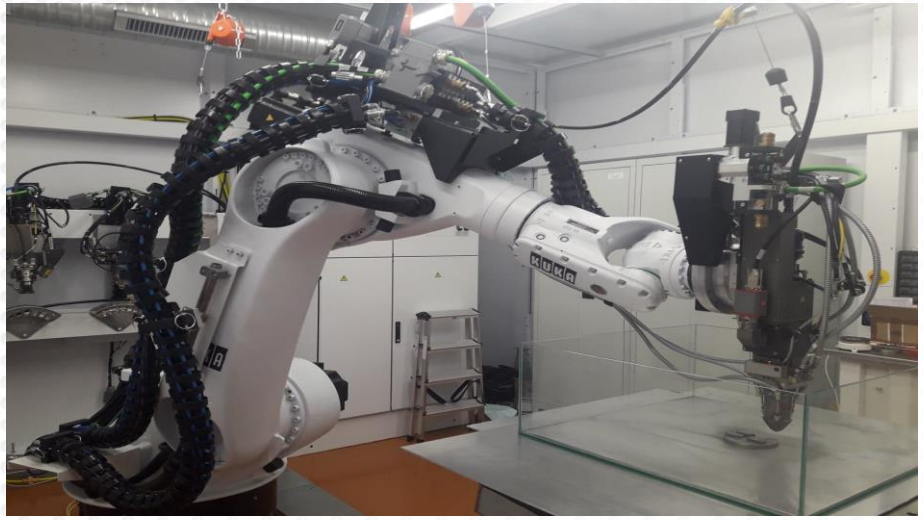

(TruDisk 3001, Trumpf, Ditzingen, Germany)

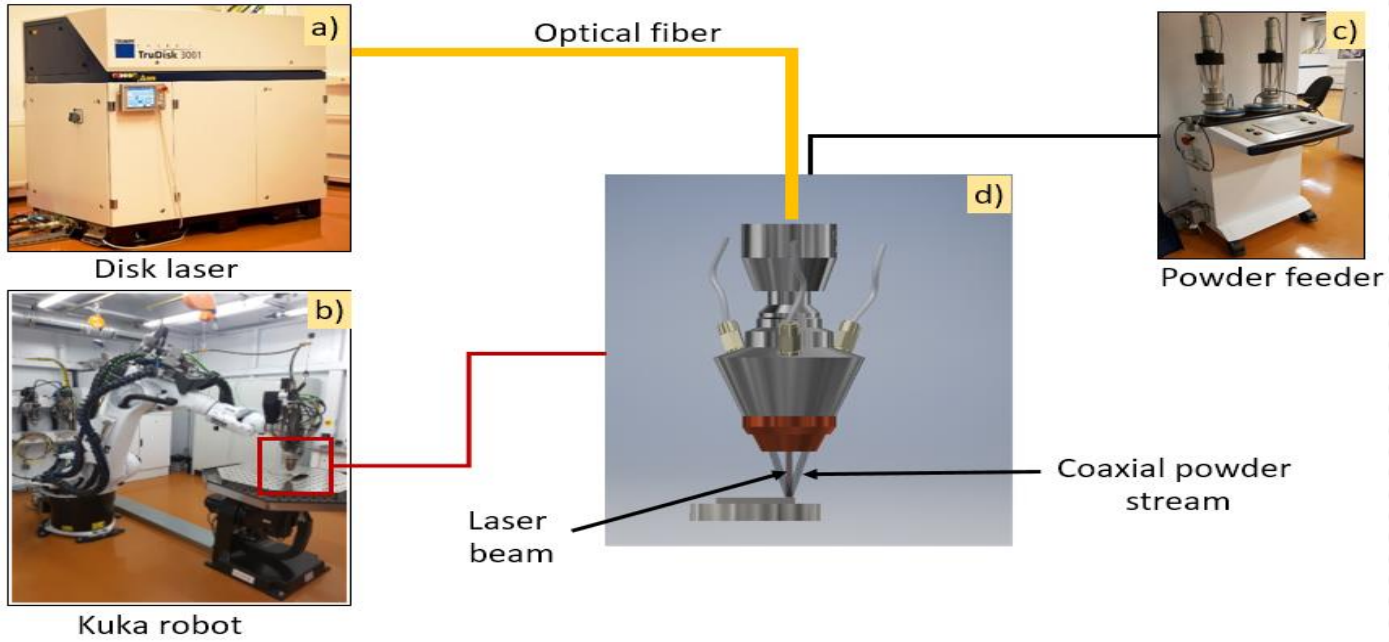

Specifications:

- Yb:YAG laser source (@1030 nm)
- Continuous and pulsed mode
- Focused top-hat laser beam spot of 800 µm
- Laser power: 300 W to 3 KW

Experimental conditions: AISI304 stainless steel substrate and powder debits

Sample No.	Laser power (P) (W)	Laser scanning speed (V_s) (m/s)	Powder feeding rate (M_p) (g/min)	Carrier gas pressure (He / Ar) (bar)	No. of deposited tracks	Height/Width of the clad (mm)	Parameters	Value
01	700	0.005	3.0	3.0 / 7.0	1.0	0.42 / 2.41	Laser absorption	0.32
02	700	0.015	3.0			0.38 / 2.12	Powder nozzle radius	2 mm
03	700	0.025	3.0			0.32 / 1.94	Length of the clad	100 mm
04	500	0.005	2.0			0.10 / 1.42	Room temperature	20 °C
05	500	0.005	3.0			0.15 / 1.59	Laser spot size	800 µm
06	500	0.005	5.0			0.19 / 1.74		
07	500	0.015	5.0			0.47 / 2.68		
08	700	0.015	5.0			0.58 / 2.97		
09	900	0.015	5.0			0.64 / 3.15		

SEM images

Three primary types of grain structures:

1) Quasi-continuous circular (QCC)
2) Long lath-shaped (LLS)
3) Combination of QCC and LLS

- Grains change from QCC to LLS when increasing laser scanning speed ***(01-03)***
- Grains transform from QCC+LLS to QCC when increasing powder flow rate ***(04-06)***
- Microstructures convert from QCC to QCC+LLS when increasing laser power ***(07-09)***

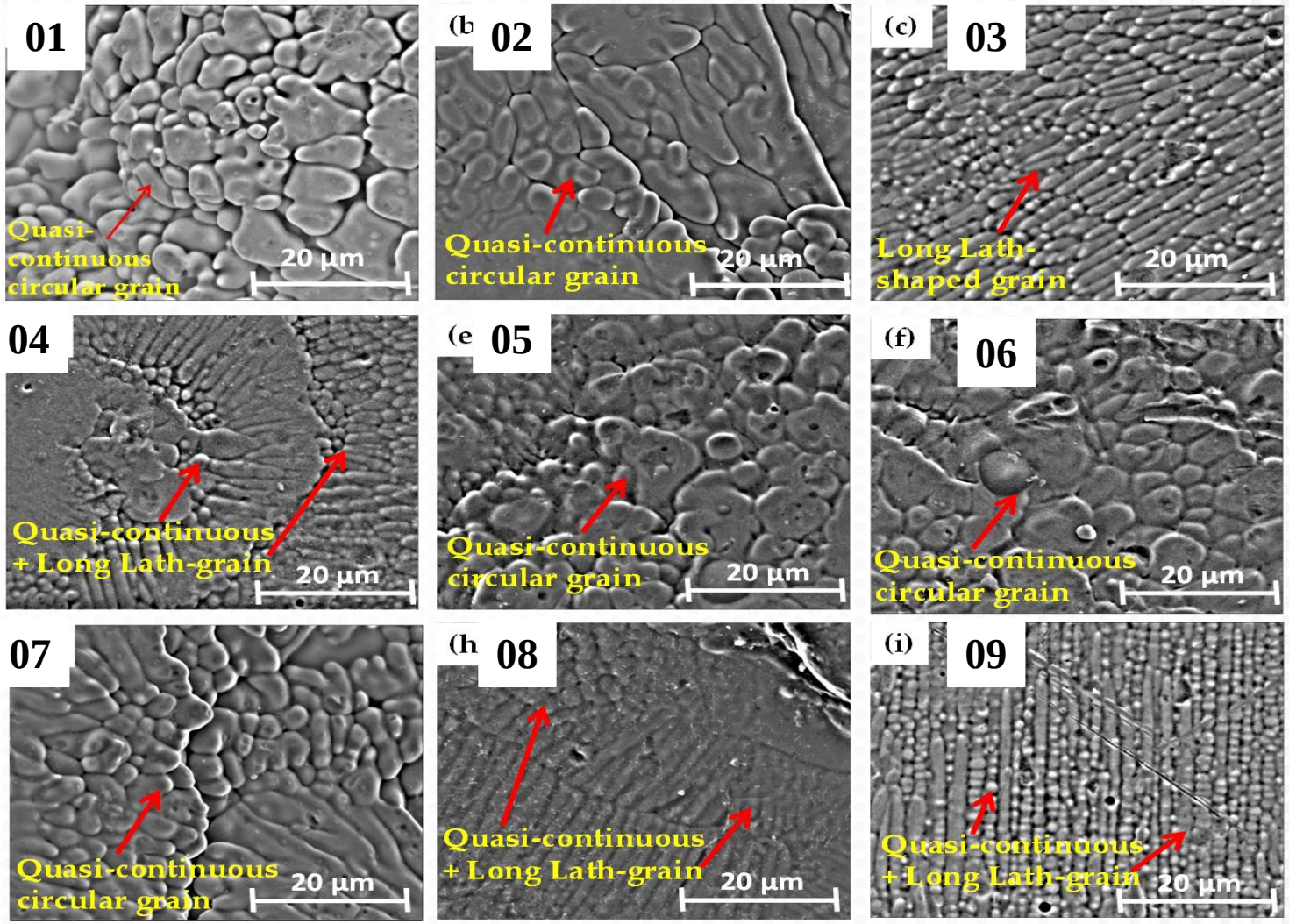

Strategy for model development

Estimated thermal history of deposited layer

Thermal stresses and strain rates in deposited layer

Johnson-Mehl-Avrami-Kohnogorov (JMAK) model:

- *Average grain size after crystallization*

Mechanical properties using average grain size:

- *Hardness*
- *Yield strength and ultimate tensile strength using hardness*

Effect of primary operating parameters on temperature history and thermal stresses

- An increase in laser power raises the absorbed energy per unit volume, resulting in higher temperature and thermal stresses (a)
- Laser scanning speed and powder flow rate are in inverse relation with temperature and thermal stresses (b and c)

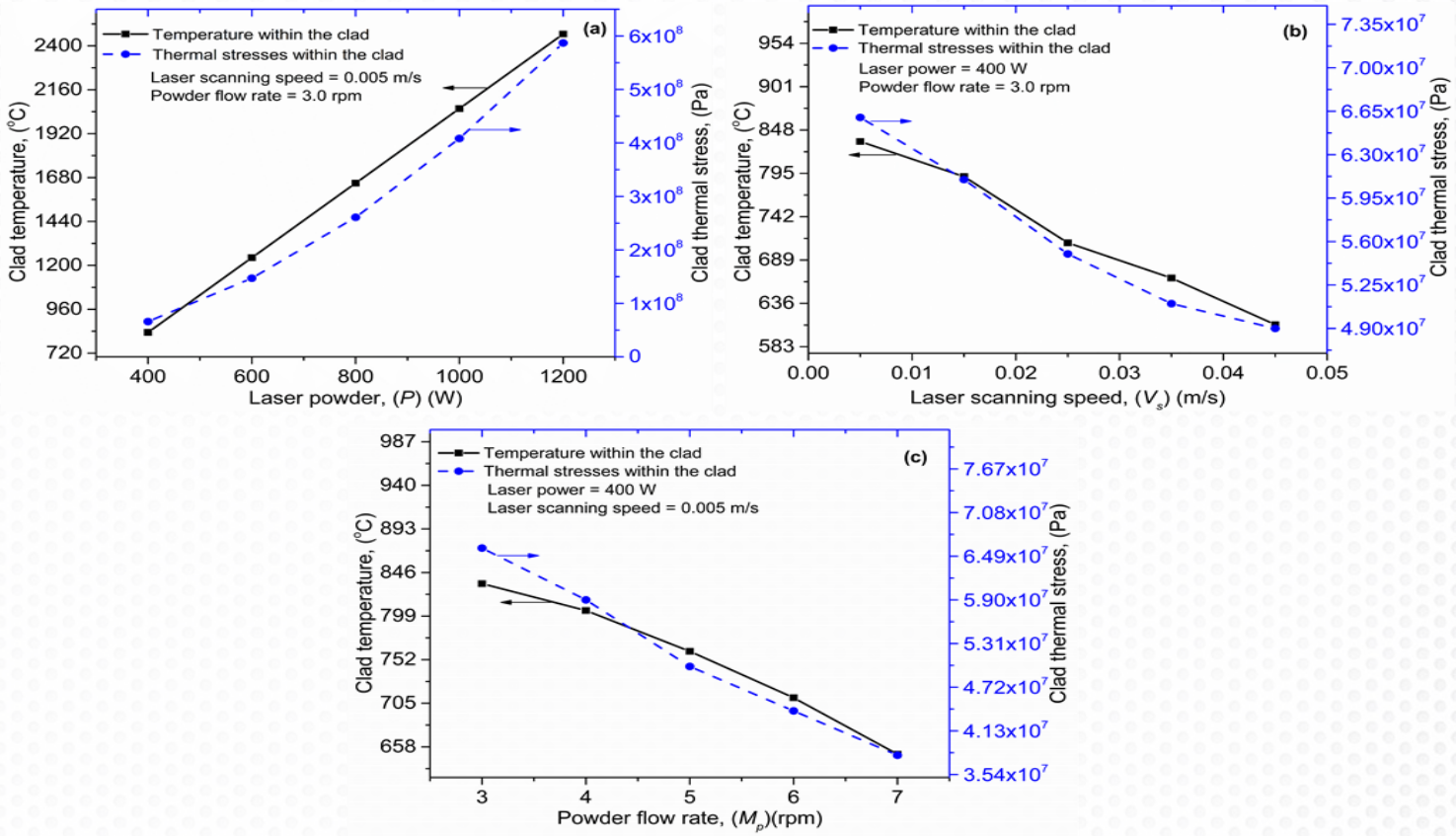

Effect of primary operating parameters on the number and average grain size

- when *laser scanning speed* or *power* decrease ⟹ *coarse grains* (a and c)
- An increment in *powder flow rate* ⟹ *refined grains* (b)
- *number of average grains* and *average grain* size inverse to each other (ASTM)

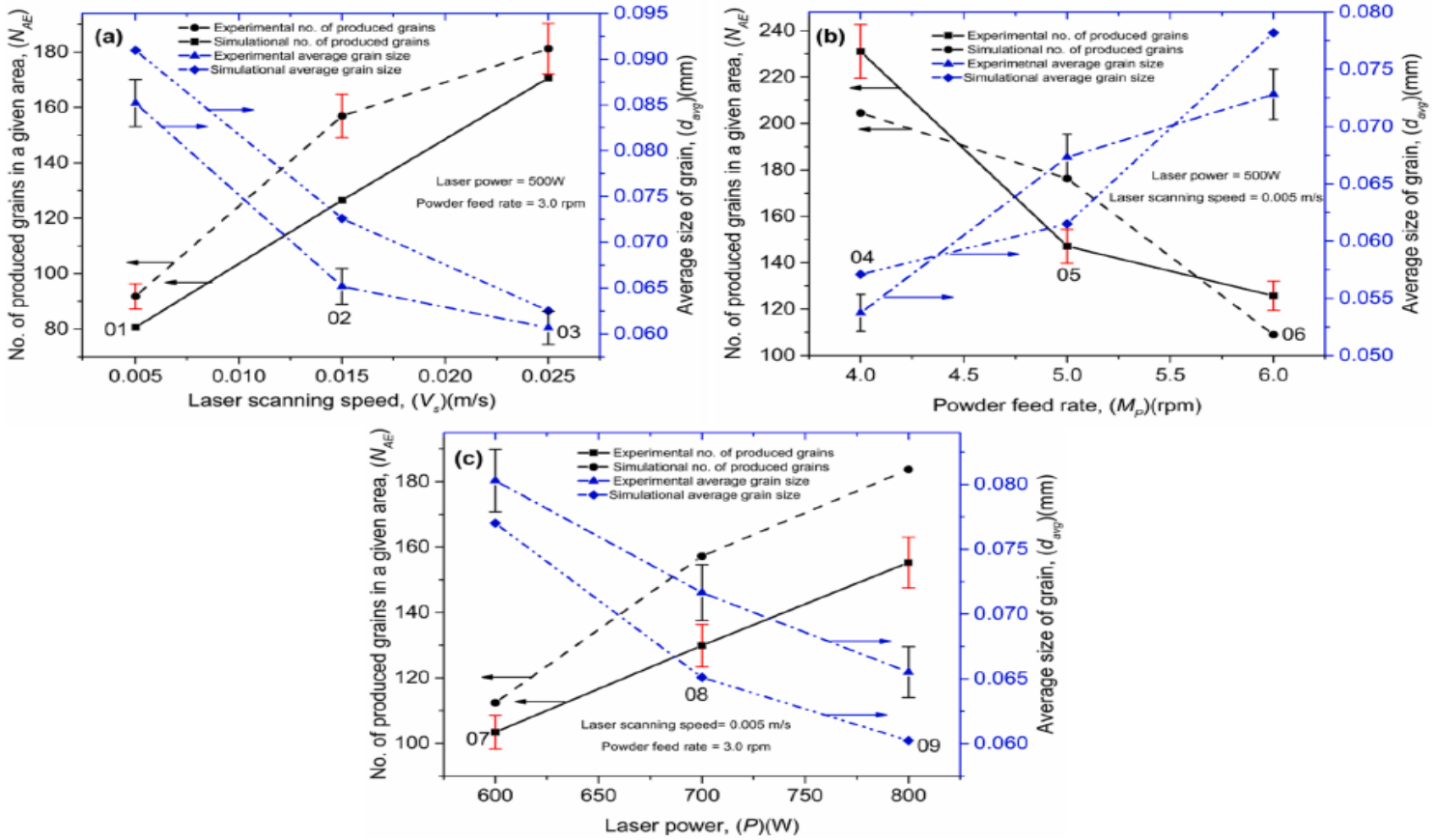

Influence of average grain size on estimated (a) ultimate tensile and yield strengths, and (b) hardness

- Smaller grains decrease the dislocations density and release the residual stresses, improving the mechanical properties (a)
- Ultimate tensile and yield strengths estimated using hardness values

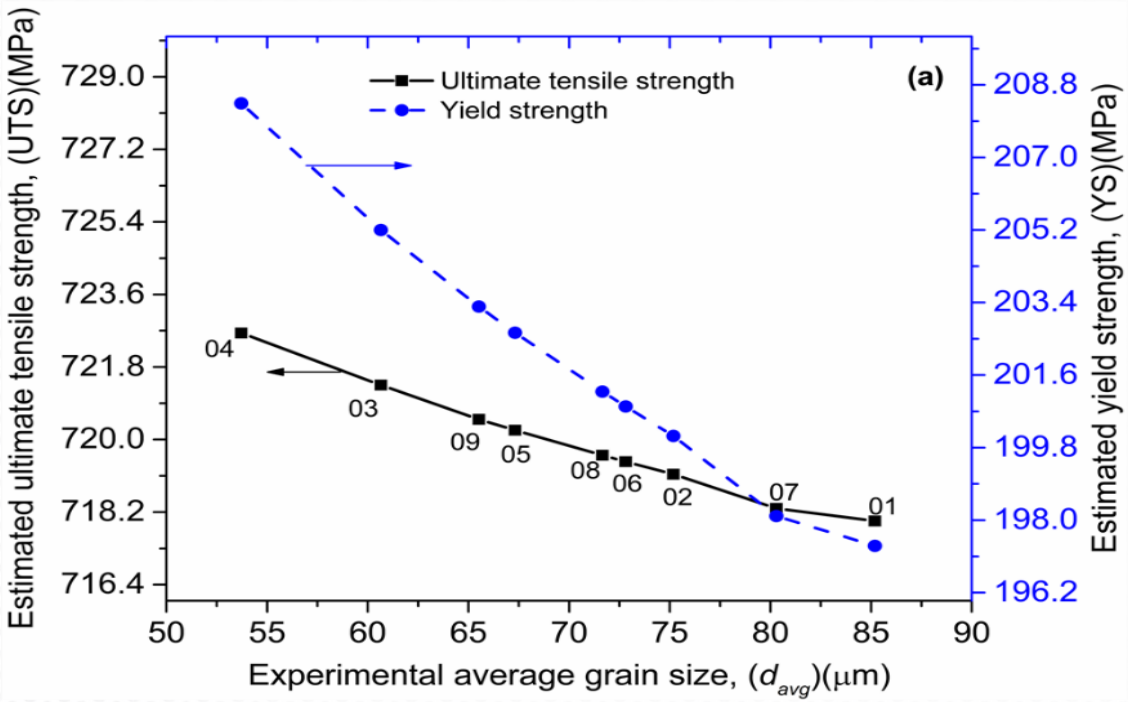

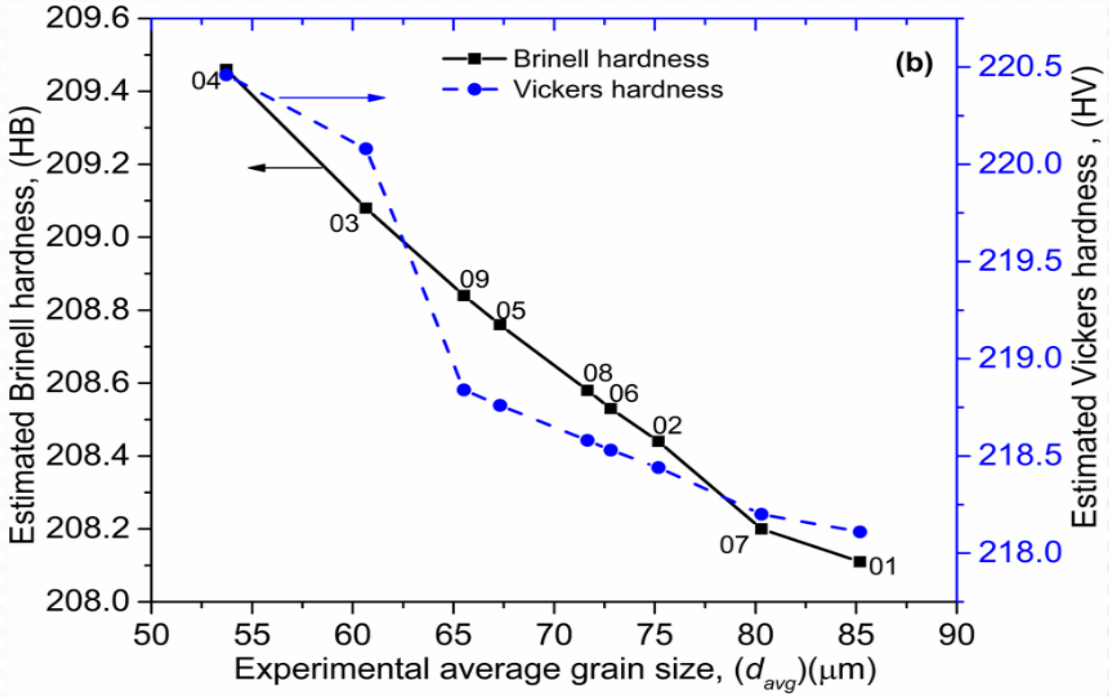

Comparison between theoretical and experimental (Vickers hardness tests)

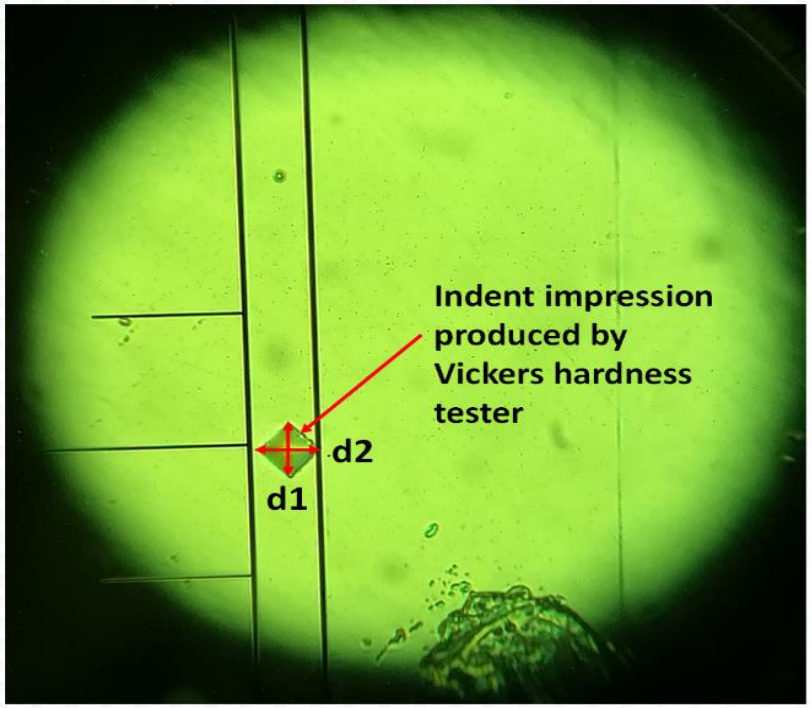

Optical image of a rhomboidal imprint of a Vickers tester with d1 and d2 diagonals

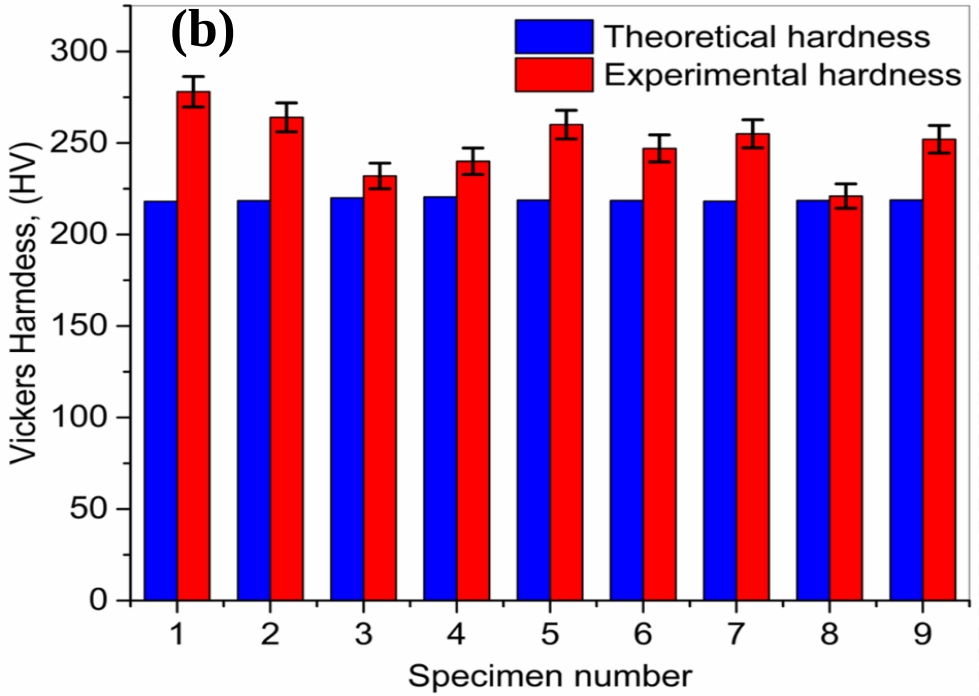

Relatively close correlation between experiments and simulations within the range of (8-10) % mean absolute deviation

Conclusions

- Analytical models have been developed for the thermal distribution inside deposited layers and for the microstructure evolution effects on mechanical properties, and porosity status in case of laser additive manufacturing.

- Simulation results were compared to experimental data and a close correlation was noticed between results, within a deviation of (4-15) % . Extensive calculations were carried out for stainless steel and confirmed in case of other metals but also ceramics, in either bulk or powder states.

- One may therefore conclude that the model could be extended to conduct time- and cost-effective guiding of functional, efficient laser additive manufacturing processing applications.

List of publications

- Grain-based morphological simulation via fractal theory with experimental verification and corresponding optical properties in laser melting deposition additive manufacturing: A demystified approach; M.A. Mahmood; A.U. Rehman; K. Ishfaq; A.C. Popescu; M. Bojan; I.N. Mihailescu; APPLIED MATHEMATICAL MODELLING
- Advances in Laser Additive Manufacturing of Cobalt-Chromium Alloy Multi-Layer Mesoscopic Analytical Modelling with Experimental Correlations: From Micro-Dendrite Grains to Bulk Objects; M.A. Mahmood; A.U. Rehman; C. Ristoscu; M. Demir; G. Popescu-Pelin; F. Pitir; M.U. Salamci; I.N. Mihailescu; NANOMATERIALS
- Laser additive manufacturing of Co-Cr alloy and the induced defects thereof; M.A. Mahmood ; A.U. Rehman; M. Lungu; F. Pitir; M.U. Salamci ; C. Ristoscu; I. Tiseanu ; I.N. Mihailescu; INTERNATIONAL JOURNAL OF ADVANCED MANUFACTURING TECHNOLOGY
- Laser additive manufacturing of bulk and powder ceramic materials: mathematical modeling with experimental correlations; M.A. Mahmood; A.C. Popescu; M. Oane; C. Ristoscu; I.N Mihailescu; RAPID PROTOTYPING JOURNAL
- Laser Coatings via State-of-the-Art Additive Manufacturing: A Review; M.A. Mahmood; A. Banica; C. Ristoscu; , N. Becherescu; I.N. Mihailescu; COATINGS
- Spatter Formation and Splashing Induced Defects in Laser-Based Powder Bed Fusion of AlSi10Mg Alloy: A Novel Hydrodynamics Modelling with Empirical Testing.; A.U. Rehman, A.M. Mahmood, P. Ansari, M. U. Salamci, A.C. Popescu, I.N. Mihailescu; METALS

List of publications

- Laser Melting Deposition Additive Manufacturing of Ti6Al4V Biomedical Alloy: Mesoscopic In-Situ Flow Field Mapping via Computational Fluid Dynamics and Analytical Modelling with Empirical Testing; M.A. Mahmood, A.U. Rehman, F. Pitir, M. U. Salamci, I. N. Mihailescu; MATERIALS
- Non-Destructive X-ray Characterization of a Novel Joining Method Based on Laser-Melting Deposition for AISI 304 Stainless Steel; M.A. Mahmood , D. Chioibasu, S. Mihai, M. Iovea, I. N. Mihailescu, A.C. Popescu; MATERIALS
- Thermal Nonlinear Klein-Gordon Equation for Nano-/Micro-Sized Metallic Particle-Attosecond Laser Pulse Interaction; M. Oane; M.A. Mahmood; A.C. Popescu; A. Banica; C. Ristoscu; I.N. Mihailescu; MATERIALS
- Artificial Neural Network Algorithms for 3D Printing; M.A. Mahmood; A.I. Visan; C. Ristoscu; I.N. Mihailescu; MATERIALS
- Mesoscopic Computational Fluid Dynamics Modelling for the Laser-Melting Deposition of AISI 304 Stainless Steel Single Tracks with Experimental Correlation: A Novel Study; A.U. Rehman; M.A. Mahmood; F. Pitir; M.U. Salamci; A.C. Popescu; I.N. Mihailescu; METALS
- Keyhole formation by laser drilling in laser powder bed fusion of Ti6Al4V biomedical alloy: mesoscopic computational fluid dynamics simulation versus mathematical modelling using empirical validation.; A. U. Rehman, M. A. Mahmood, F. Pitir, M. U. Salamci, A. C. Popescu, I. N. Mihailescu; NANOMATERIALS

Questions and Answers are welcomed!